ChemComm

COMMUNICATION

View Article Online
View Journal | View Issue

Cite this: *Chem. Commun.*, 2016, 52, 3344

Received 11th January 2016,
Accepted 20th January 2016

DOI: 10.1039/c6cc00267f

www.rsc.org/chemcomm

Enhanced product selectivity promoted by remote metal coordination in acceptor-free alcohol dehydrogenation catalysis†

Marta Valencia,[ab] Helge Müller-Bunz,[b] Robert A. Gossage[ac] and Martin Albrecht*[ab]

A bimetallic $[Ir^{3+}]_2$ complex was synthesized based on a bridging 1,2,3-triazole ligand that coordinates to one Cp*Ir unit as *N*,*N*-bidentate chelate, and to the other as a *C*,*C*-bidentate ligand. When compared to monometallic homologues, the bimetallic complex shows greatly enhanced product selectivity for the acceptorless dehydrogenation of alcohols; spectroscopic and electrochemical analysis suggest significant alteration of the metal properties in the bimetallic system compared to the monometallic species, which offers a rationale for the observed high selectivity.

Nature achieves high selectivity and reactivity in substrate activation by the application of highly complex molecular enzymes. Many of these systems rely on cooperation between reactive metal centres.[1] These metal sites are often arranged in close mutual proximity, in particular in cases where redox chemistry is involved. This necessity is governed by the typical requirement for two-electron transformations that involve bio-available metals with one-electron redox processes as the only energetically feasible option (*e.g.* $Cu^{+/2+}$, $Fe^{2+/3+}$).[2] In synthetic systems, judicious ligand design allows the two redox active metal centres to be placed in an enforced proximity. In many cases, this leads to metal–metal bond formation during the redox processes. Hence the influence of one or both metals on one another is intimately connected.[3] Less well-known are catalytic systems in which redox active metals are held in a conformation that inhibits metal–metal bond formation.[4] Elegant work by Peris using 1,2,4-triazolylidene scaffolds revealed a direct positive effect on catalytic performance.[5] Here, we present a bimetallic system that induces greatly enhanced product selectivity when compared to the monometallic homologues, in parts through effective kinetic discrimination. Efficient alteration of the metal properties are demonstrated *inter alia* by a significant lowering of the potential for iridium(III) oxidation.

We previously reported on the excellent catalytic activity of iridium complexes in oxidation reactions, which is imparted by the unique features of mesoionic triazolylidene ligands[6] containing pyridyl-derived substituents.[7] Inspired by these results, we have now investigated Cp*Ir complexes of related ligands containing secondary bonding capabilities (Cp* = pentamethylcyclopentadienyl, $C_5Me_5^-$). To this end, 1,2,3-triazole containing two pyridyl substituents at N1 and C4 positions was selectively monomethylated at the C-bound pyridyl site to afford the pyridinium triazole ligand precursor **L1** (ESI†). Metalation of this pyridinium salt with $[IrCp^*Cl_2]_2$ in the presence of NaOAc at room temperature induced C_{trz}–H bond activation and subsequent cyclometalation to afford the bimetallic complex **1** (Scheme 1).[8] This complex was air-stable and purified by column chromatography, and was isolated as a red solid in 48% yield. Note that complex **1** contains two non-identical iridium centers in formal +3 oxidation

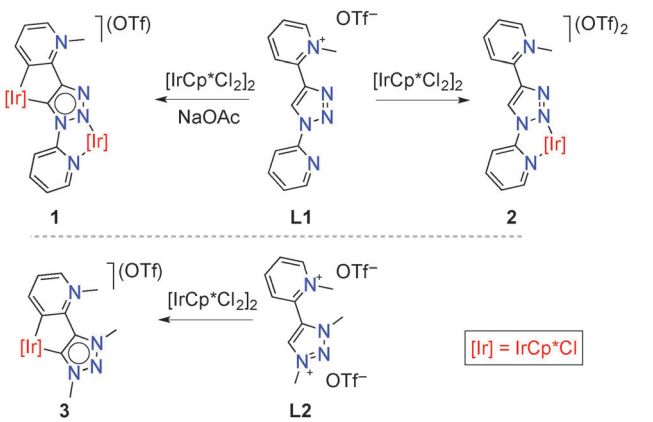

Scheme 1 Synthesis of the bis-iridium complex **1**, and its monometallic analogues **2** and **3**.

[a] *Departement für Chemie und Biochemie, Universität Bern, Freiestrasse 3, CH-3012 Bern, Switzerland. E-mail: martin.albrecht@dcb.unibe.ch*
[b] *School of Chemistry, University College Dublin, Belfield, Dublin 4, Ireland*
[c] *Department of Chemistry & Biology, Ryerson University, 350 Victoria St., Toronto, ON M5B 2K3, Canada*

† Electronic supplementary information (ESI) available: Synthetic procedures, representative catalytic runs and time conversion profiles, crystallographic details. CCDC 1434920 (**1**) and 1434921 (**2**). For ESI and crystallographic data in CIF or other electronic format see DOI: 10.1039/c6cc00267f

state, one κ^2-*N*,*N*′ bound and the second displaying a κ^2-*C*,*C*′ bonding motif; one of these bonding pockets is formally anionic.[9]

Treatment of the pyridinium salt **L1** with $[IrCp^*Cl_2]_2$ under identical conditions but in the absence of NaOAc yielded the monometallic complex **2** (Scheme 1), which was isolated as a light yellow solid (61%). While the N3 position of the triazole heterocycle is generally more basic and hence should coordinate preferably to a Lewis acid,[10] chelation *via* bonding to the pyridyl unit directs the metal to the triazole N2-position. Related metal coordination to N2 in triazolium salts has been established in specific cases, in particular when chelating groups were available as substituents.[11] Notably, complex **2** contains an iridium center in essentially the same coordination environment as the *N*,*N*-bound iridium center in complex **1**. The *C*,*C*-bound portion of complex **1** is mimicked by the previously reported[7b] complex **3** featuring a mesoionic pyridylidene and a mesoionic triazolylidene ligand bonding site (Scheme 1). Even though the ligand in complex **1** is formally an anionic L,X-type system, previous work provides evidence that *N*-coordination of metal centers to *N*-heterocycles such as triazoles or imidazoles has very similar effects to *N*-alkylation.[12] In both complexes, the triazole-derived heterocycle is mesoionic in nature, and hence complex **3** is a better mimic of the *C*,*C*-chelated iridium center than a rigidly anionic triazolyl ligand site. In support of this notion, the triazol proton resonance shifts by about the same shift difference when the triazole scaffold is alkylated or coordinating to iridium.[13]

Complexes **1–3** were identified by elemental analysis, ^{1}H and ^{13}C NMR spectroscopy, and single crystal X-ray diffraction (ESI†). The integral ratio of the Cp-bound CH_3 groups relative to the singlet of the pyridinium–CH_3 resonance gave unambiguous evidence for the presence of two and one [Ir(Cp*)] units per ligand site in complexes **1** and **2**, respectively. While pyridylidene and triazolylidene bonding was readily deduced from the multiplicity and chemical shift of the pyridylidene ^{1}H resonances and ^{13}C NMR data (*e.g.* δ_C = 160.4 for C_{trz}–Ir, δ_C = 160.7 for C_{py}–Ir), *C*,*C*-chelation was established unambiguously by X-ray diffraction (Fig. 1). Structural comparison reveals that the Ir–C bonds are consistently shorter than the Ir–N bonds, irrespective of the type of heterocycle (trz or pyr; Table 1). The Ir–N and the Ir–C bond lengths of **1** are essentially identical to the corresponding bond lengths in the monometallic analogues **2** and **3**, suggesting that complexes **2** and **3** are appropriate structural mimics for the two different iridium centers in complex **1**.

Complexes **1–3** were used as catalyst precursors for the acceptorless oxidation of alcohols[14] using benzyl alcohol as a model substrate. Reactions were typically carried out at 150 °C and using 5 mol% [Ir] in 1,2-dichlorobenzene as solvent (Table 2 and Fig. S1, ESI†). Evaluation of these catalytic runs indicates two important and unusual features. Firstly, the initial catalytic activity as well as the alcohol conversion after 24 h are higher for both monometallic complexes **2** and **3** than that of the bimetallic Ir_2 complex **1**. For example, conversions after 24 h reach 89% and 98% with the *N*,*N*-bidentate and *C*,*C*-bidentate coordinated iridium centers, respectively, in a monometallic framework, while the bimetallic system only reaches 72% within the same period and at the same concentration of iridium (entries 1–4). Full conversion requires longer reaction times (entry 2). Secondly and more significantly, complete product selectivity towards benzyl aldehyde is obtained using the bimetallic catalyst precursor **1** and conversions and yields are identical even after complete substrate conversion (up to 4 d). In sharp contrast, the monometallic complexes **2** and **3** both afforded a mixture of two products, *viz.* benzaldehyde from dehydrogenation and, in about equal portions, dibenzyl ether as a result of alcohol dehydration. Similar etherification has been noted with related complexes.[15] Of note, runs involving a combination of complex **2** and **3** (2.5 mol% of each complex to obtain the same 5 mol% loading) under the same catalytic conditions yielded essentially identical results as if only one of the mono-Ir complexes is employed, that is, higher activity yet vastly inferior selectivity than **1** (entry 5).[16] We thus attribute the remarkably high selectivity of the catalyst derived from complex **1** to the unique electronic configuration imparted by the presence of two metal centers. This bimetallic configuration effectively suppresses dehydration and decelerates also dehydrogenation, thus producing benzaldehyde at lower rate, but with exquisite selectivity.

Table 1 Selected bond lengths (Å) and angles (°) for **1–3**[a]

2		**1**			**3**[b]
2.080(5)	Ir–N_{trz}	2.072(2)	1.993(2)	Ir–C_{trz}	2.017(1)
2.116(6)	Ir–N_{py}	2.116(6)	2.049(2)	Ir–C_{py}	2.049(1)
2.396(2)	Ir–Cl	2.4039(6)	2.4088(4)	Ir–X[a]	2.033(2)
75.5(2)	N_{trz}–Ir–N_{py}	75.53(7)	77.32(2)	C_{trz}–Ir–C_{py}	76.02(2)
84.1(2)	Cl–Ir–N_{trz}	84.69(5)	91.57(6)	X–Ir–C_{trz}	90.09(6)
87.8(2)	Cl–Ir–N_{py}	84.60(5)	89.39(6)	X–Ir–C_{py}	87.61(6)

[a] X = Cl in complex **1**, X = NCMe in complex **3**. [b] From ref. 7*b*.

Table 2 BnOH oxidation catalyzed by iridium complexes **1–3**[a]

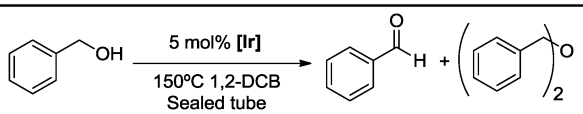

Entry	[Ir]	Time (h)	Conv'n[b] (%)	BnCHO/Bn_2O[c] (%)
1	**1**	24	72	100/0
2	**1**	96	95	100/0
3	**2**	24	89	42/58
4	**3**	24	98	57/43
5	**2** + **3**[d]	24	92	46/54

[a] Conditions: alcohol (0.2 mmol), [Ir] (0.01 mmol, 5 mol% based on Ir), 1,2-dichlorobezene (2 mL), 150 °C. [b] Determined by ^{1}H NMR spectroscopic analysis in $CDCl_3$ with hexamethylbenzene as internal standard. [c] Ratio of products given in percent. [d] 5 μmol of **2** plus 5 μmol of **3**.

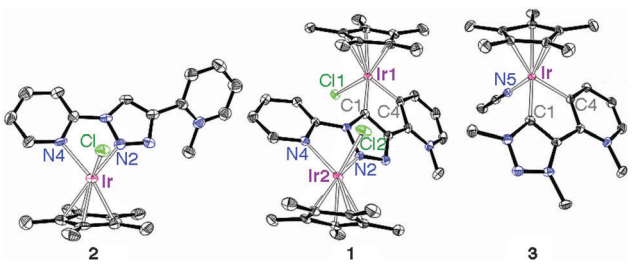

Fig. 1 ORTEP representation of complexes **1–3** (50% probability, hydrogens and non-coordinated OTf^- anions omitted for clarity).

To shed some light on the unique selectivity of the bimetallic complex **1**, the spectroscopic and physical properties of **1–3** were examined in more detail. Structural (ground-state) comparison of bimetallic **1** to both monometallic complexes **2** and **3** reveals little significant differences (see X-ray data above). The ^{1}H NMR spectrum (CD_2Cl_2) of complex **1** shows two singlet resonances for the two magnetically inequivalent Cp* ligands (δ_H = 1.83 and 1.60). The lower field singlet resonates at a similar frequency to that observed for both complexes **2** and **3** (δ_H = 1.82 and 1.84, respectively), whereas the higher field singlet indicates a significantly more shielded environment of one IrCp* unit. Nuclear Overhauser experiments unambiguously demonstrated that the shielded Cp* unit belongs to the *C*,*C*-bidentate coordinated ligand,[17] thus offering a rationale for the altered catalytic activity and selectivity, and suggesting that the triazolylidene-bound iridium is the catalytically active site.

The UV-vis spectra of complexes **1–3** (CH_2Cl_2: Fig. 2) revealed notable differences between the nature of complex **1** with respect to that of **2** or **3**. The monometallic complexes **2** or **3** feature only a single absorption band at 288 or 326 nm, respectively, while complex **1** displays three absorption bands, which are clearly not simple superimpositions of the bands of complexes **2** and **3**. Most relevant is the new charge transfer band at 460 nm, which has no counterpart in the monometallic complexes. Presumably, the planar organization of the three heterocycles in complex **1**, entailed by the coordination to two iridium centers, increases the donor properties and thus enhance LMCT interactions. The intra-ligand charge transfer bands (π–π^* transitions) have energies that are similar to those observed in the monometallic complexes and are located at 324 and 260 nm (*cf.* 326 and 288 nm for **3** and **2**, respectively).

Probably the most remarkable feature of the bimetallic complex **1** is the fully reversible oxidation process as established by electrochemical studies using cyclic voltammetry (CV; Fig. 3). While no oxidation wave is observed in either complex **2** nor **3**, a reversible single-electron oxidation process is present in the bimetallic complex **1** at $E_{1/2}$ = + 1.03 V *vs.* SCE. Cathodic and anodic peak currents are essentially equal at various scan rates (see Fig. S3 and Table S2, ESI†). The complete lack of redox behavior of both monometallic complexes **2** and **3** is unsurprising[18] and

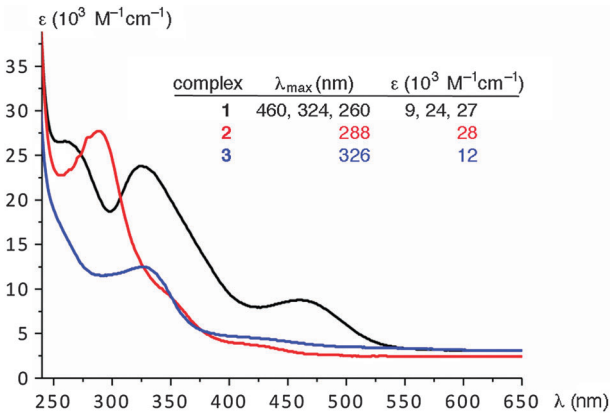

Fig. 2 UV/vis spectra of complexes **1–3** (in CH_2Cl_2, *ca.* 10^{-5} M).

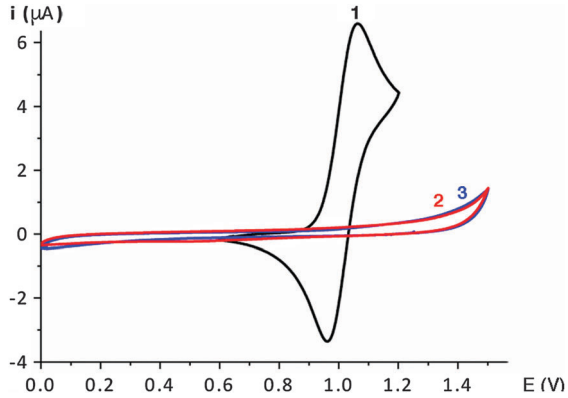

Fig. 3 Cyclic voltammogram of complexes **1–3** in CH_2Cl_2 (*ca.* 10^{-3} M) with Ag/AgCl (3 M) as reference and ferrocene as internal standard ($E_{1/2}$ (Fc/Fc$^+$) = 0.46 V *vs.* SCE). Complex **1**: $E_{1/2}$ = 1.03 V, $I_{pa} \approx I_{pc}$.

effectively negates ligand-centered redox processes,[19] thus demonstrating the high redox stability of the ligand framework and of the formal +3 oxidation state of the iridium center in both complexes. In contrast, the fully reversible nature of the one-electron redox cycle of complex **1** likely involves the *C*,*C*-chelated iridium center and thus corroborates the UV-vis behaviour and the higher electron density as surmised from NMR spectroscopy. Considering the otherwise high similarity of the iridium centers in complex **1** with those of the monometallic complexes **2** and **3**, we suggest that the electronic configuration imparted by the *N*,*N*-bound iridium center significantly affects the electronic properties of the *C*,*C*-bound iridium site, and thus likely constitutes a primary reason for the observed catalytic selectivity.

The high selectivity towards alcohol dehydrogenation imparted by complex **1** was further examined with a small selection of representative primary and secondary alcohols (Table 3). In all cases, the ketone/aldehyde is the exclusive product and no traces of the corresponding ether was detected that would point to dehydration activity (Fig. S2, ESI†). Hence high product selectivity is an intrinsic feature of the bimetallic triazolylidene complex **1**. Substrate variation suggests that aromatic substituents enhance the catalytic activity (entries 1–3 *vs.* entries 4 and 5), and that secondary alcohols are faster converted than primary alcohols (*e.g.* entry 1 *vs.* 3, or 4 *vs.* 5). Specifically, phenylethanol and

Table 3 Alcohol oxidation screening catalyzed by **1**[a]

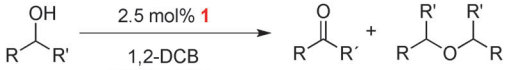

Entry	R	R′	Time (h)	Conv'n[b] (%)	Ketone/ether[c] (%)
1	Ph	CH_3	24	89	100/0
2	Ph	Ph	24	80	100/0
3	Ph	H	24	72	100/0
4	Et	CH_3	24	70	100/0
5	*n*Oct	H	24	37	100/0

[a] Conditions: alcohol (0.2 mmol), complex **1** (0.01 mmol, 2.5 mol%, 5 mol% based on Ir), 1,2-dichlorobezene (2 mL), 150 °C. [b] Determined by ^{1}H NMR spectroscopic analysis with hexamethylbenzene as internal standard. [c] % of product ratio.

diphenylmethanol are easier dehydrogenated (89% and 80% yield, entries 1 and 2) than benzylalcohol (72%, entry 3). Aliphatic alcohols such as 2-butanol produced the corresponding ketone in 70% yield (entry 4). Using primary and aliphatic alcohols such as 1-octanol afford the lowest conversion (37%, entry 5). These results indicate that the selectivity can be tailored even further to differentiate effectively between aliphatic primary and aromatic secondary alcohols.

In conclusion, a bimetallic $[Ir^{3+}]_2$ complex containing a bridging triazolylidene ligand has been developed. This bimetallic complex displays superior catalytic selectivity for the acceptorless dehydrogenation of alcohols when compared to closely related monometallic analogues. Spectroscopic and electrochemical analyses reveal a unique electronic setting of the *C*,*C*-bound iridium center that is imparted by the *N*,*N*-coordinated metal unit, and these features presumably entail the high selectivity. When considering the slightly lower reaction rates, it is plausible that the high selectivity originates from an effective suppression of the dehydration pathway, which results in lower activity, yet higher selectivity. Cooperative substrate binding is less probable when considering the activity of the monometallic complexes. While synergistic interactions have been known to provide access to enhanced catalytic activity, the effects on product selectivity are much less developed and the results presented here may stimulate further work along these lines.

The authors gratefully acknowledge financial support from the European Commission (ERC CoG 615653, Marie Sklodowska-Curie Action 660929 to M. V.).

Notes and references

1 (*a*) S. J. Lippard and J. M. Berg, *Principles of Bioinorganic Chemistry*, University Science Books, Mill Valley, CA1994; (*b*) A. Sigel, H. Sigel and R. K. O. Sigel, *Metal Ions in Life Science*, Royal Society of Chemistry, London, UK, 2009; (*c*) E. I. Solomon, R. K. Szilagyi, S. DeBeer George and L. Basumallick, *Chem. Rev.*, 2004, **104**, 419; (*d*) E. I. Solomon, M. J. Baldwin and M. D. Lowery, *Chem. Rev.*, 1992, **92**, 521.

2 (*a*) N. Sträter, W. N. Lipscomb, T. Klabunde and B. Krebs, *Angew. Chem., Int. Ed. Engl.*, 1996, **35**, 2024; (*b*) H. Steinhagen and G. Helmchen, *Angew. Chem., Int. Ed. Engl.*, 1996, **35**, 2339; (*c*) R. G. Wilkins, *Chem. Soc. Rev.*, 1992, **21**, 171; (*d*) J. B. Vincent, G. L. Olivier-Lilley and B. A. Averill, *Chem. Rev.*, 1990, **90**, 1447.

3 For selected examples, see: (*a*) P. Buchwalter, J. Rosé and P. Braunstein, *Chem. Rev.*, 2015, **115**, 28; (*b*) S. M. Inamdar, V. S. Shinde and N. T. Patil, *Org. Biomol. Chem.*, 2015, **13**, 8116; (*c*) J. A. Mata, F. E. Hahn and E. Peris, *Chem. Sci.*, 2014, **5**, 1723; (*d*) N. P. Mankad, *Synlett*, 2014, 1197; (*e*) L. Stegbauer, F. Sladojevich and D. J. Dixon, *Chem. Sci.*, 2012, **3**, 942; (*f*) J. I. van der Vlugt, *Eur. J. Inorg. Chem.*, 2012, 363; (*g*) M. Delferro and T. J. Marks, *Chem. Rev.*, 2011, **111**, 2450; (*h*) H. Li and T. J. Marks, *Proc. Natl. Acad. Sci. U. S. A.*, 2006, **103**, 15295; (*i*) M. Shibasaki, M. Kanai, S. Matsunaga and N. Kumagai, *Top. Organomet. Chem.*, 2011, **37**, 1; (*j*) N. Kielland, E. C. Escudero-Adán, M. Martínez Belmonte and A. W. Kleij, *Dalton Trans.*, 2013, **42**, 1427; (*k*) U. J. Schele, S. Dechert and F. Meyer, *Chem. – Eur. J.*, 2008, **14**, 5112; (*l*) S. W. Gersten, G. J. Samuels and T. J. Meyer, *J. Am. Chem. Soc.*, 1982, **104**, 4029; (*m*) C. Sens, I. Romero, M. Rodriguez, A. Llobet, T. Parella and J. Benet-Buchholz, *J. Am. Chem. Soc.*, 2004, **126**, 7798; (*n*) P. Haack and C. Limberg, *Angew. Chem., Int. Ed.*, 2014, **53**, 4282.

4 (*a*) S. Sabater, J. A. Mata and E. Peris, *Organometallics*, 2012, **31**, 6450; (*b*) M. Nussbaum, O. Schuster and M. Albrecht, *Chem. – Eur. J.*, 2013, **19**, 17517.

5 (*a*) A. Zanardi, J. A. Mata and E. Peris, *J. Am. Chem. Soc.*, 2009, **131**, 14531; (*b*) S. Sabater, J. A. Mata and E. Peris, *Nat. Commun.*, 2013, **4**, 3553.

6 (*a*) P. Mathew, A. Neels and M. Albrecht, *J. Am. Chem. Soc.*, 2008, **130**, 13534; (*b*) G. Guisado-Barrios, J. Bouffard, B. Donnadieu and G. Bertrand, *Angew. Chem., Int. Ed.*, 2010, **49**, 4759; (*c*) J. D. Crowley, A.-L. Lee and K. J. Kilpin, *Aust. J. Chem.*, 2011, **64**, 1118; (*d*) K. F. Donnelly, A. Petronilho and M. Albrecht, *Chem. Commun.*, 2013, **49**, 1145.

7 (*a*) R. Lalrempuia, N. D. McDaniel, H. Müller-Bunz, S. Bernhard and M. Albrecht, *Angew. Chem., Int. Ed.*, 2010, **49**, 9765; (*b*) J. A. Woods, R. Lalrempuia, A. Petronilho, N. D. McDaniel, H. Müller-Bunz, M. Albrecht and S. Bernhard, *Energy Environ. Sci.*, 2014, **7**, 2316; (*c*) I. Corbucci, A. Petronilho, H. Müller-Bunz, L. Rocchigiani, M. Albrecht and A. Macchioni, *ACS Catal.*, 2015, **5**, 2714.

8 A. Petronilho, J. A. Woods, H. Mueller-Bunz, S. Bernhard and M. Albrecht, *Chem. – Eur. J.*, 2014, **20**, 15775.

9 Note that the resonance structure in Scheme 1 suggests a carbanionic triazolyl binding site, though an alternative resonance structure featuring a Ir=C carbene unit leads to a nitrogen anion and to an L,X-type *N*,*N*-bidentate coordination site.

10 J. R. Wright, P. C. Young, N. T. Lucas, A.-L. Lee and J. L. Crowley, *Organometallics*, 2013, **32**, 7065.

11 (*a*) Y. Tulchinsky, M. A. Iron, M. Botoshansky and M. Gandelman, *Nat. Chem.*, 2011, **3**, 525; (*b*) W. K. C. Lo, G. S. Huff, J. R. Cubanski, A. D. W. Kennedy, C. J. McAdam, D. A. McMorran, K. C. Gordon and J. D. Crowley, *Inorg. Chem.*, 2015, **54**, 1572; (*c*) P. Thongkam, S. Jindabot, S. Prabpai, P. Kongsaeree, T. Wititsuwannakul, P. Surawatanawong and P. Sangtrirutnugul, *RSC Adv.*, 2015, **5**, 55847.

12 This notion is supported also by the isolobal relationship of the $[CH_3]^+$ unit in **3** with the $[IrCp^*Cl]^+$ fragment in **1**. For previous evidence, see: (*a*) O. Karagiaridi, M. B. Lalonde, W. Bury, A. A. Sarjean, O. K. Farha and J. T. Hupp, *J. Am. Chem. Soc.*, 2012, **134**, 18790; (*b*) M. B. Lalonde, O. K. Farha, K. A. Scheidt and J. T. Hupp, *ACS Catal.*, 2012, **2**, 1550; (*c*) H. M. Bass, S. A. Cramer, A. S. McCullough, K. J. Bernstein, C. R. Murdock and D. M. Jenkins, *Organometallics*, 2013, **32**, 2160.

13 The triazole proton shifts typically about 0.50 ppm downfield upon *N*-methylation (see ref. 6–8). Iridium coordination to N2 shifts the Htrz resonance from δ_H = 9.39 in L1 to δ_H = 10.22 in complex **2** ($\Delta\delta$ = 0.83), suggesting a similar electronic perturbation of the heterocycle upon methylation and iridium coordination.

14 For pioneering work on acceptorless alcohol oxidation, see: (*a*) J. Zhang, M. Gandelman, L. J. W. Shimon, H. Rozenberg and D. Milstein, *Organometallics*, 2004, **23**, 4026; (*b*) H. Junge and M. Beller, *Tetrahedron Lett.*, 2005, **46**, 1031; (*c*) G. R. A. Adair and J. M. J. Williams, *Tetrahedron Lett.*, 2005, **46**, 8233for recent examples, see: (*d*) B. Saha, S. M. Wahidur Rahaman, P. Daw, G. Sengupta and J. K. Bera, *Chem. – Eur. J.*, 2014, **20**, 6542; (*e*) S. Dinda, A. Genest and N. Rösch, *ACS Catal.*, 2015, **5**, 4869; (*f*) H. Zhao, Q. Chen, L. Wei, Y. Jiang and M. Cai, *Tetrahedron*, 2015, **71**, 8725; for examples based on triazolylidene ligands, see: (*g*) A. Prades, E. Peris and M. Albrecht, *Organometallics*, 2011, **30**, 1162; (*h*) M. Delgado-Rebollo, D. Canseco-Gonzalez, M. Hollering, H. Müller-Bunz and M. Albrecht, *Dalton Trans.*, 2014, **43**, 4462.

15 (*a*) A. Prades, R. Corberan, M. Poyatos and E. Peris, *Chem. – Eur. J.*, 2008, **14**, 11474; (*b*) A. Petronilho and M. Albrecht, in preparation.

16 This result suggests that the enhanced selectivity is not due to intermolecular synergistic effects of the two iridium centers. Moreover, catalytic runs with complex **3** in the presence of 5 mol% KOH did not change the selectivity, which excludes a Brønsted acid catalyzed etherification (Table S1, ESI†). Complex **2** is unstable in the presence of base and undergoes a C–H activation process.

17 The resonance at 1.83 ppm shows a nOe with the N–CH_3 group (δ_H = 4.71), while the signal at 1.60 ppm displays a nOe with the pyridylidene C_3–H proton (δ_H = 8.53). Both Cp–CH_3 singlets show an nOe with pyridyl protons, the resonance at 1.83 ppm with C_3–H (δ_H = 8.78), the signal at 1.60 ppm with C_6–H (δ_H = 9.04).

18 A. Petronilho, A. Llobet and M. Albrecht, *Inorg. Chem.*, 2014, **53**, 12896.

19 For a recent example of oxidation involving the ligand, see: K. Jeya Prathap and G. Maayan, *Chem. Commun.*, 2015, **51**, 11096.